A Simple Triangular Element for Thick and Thin Plate and Shell Analysis

E. Oñate
F. Zarate
F. Flores

Publicación CIMNE Nº 33, Marzo 1993

A Simple Triangular Element for Thick and Thin Plate and Shell Analysis

E. Oñate
F. Zarate
F. Flores

Publicación CIMNE Nº 33, March 1993

Centro Internacional de Métodos Numéricos en Ingeniería
Gran Capitán s/n, 08034 Barcelona, España

A SIMPLE TRIANGULAR ELEMENT FOR THICK AND THIN PLATE AND SHELL ANALYSIS

E.Oñate

F. Zarate

F. Flores

Int. Center for Numerical Method in Engineering.
E.T.S. Ingenieros de Caminos, Canales y Puertos
Univ. Politécnica de Cataluña
Gran Capitán s/n, 08034 Barcelona, Spain

SUMMARY

A new plate triangle based on Reissner-Mindlin plate theory is proposed. The element has a standard linear deflection field and an incompatible linear rotation field expressed in terms of the mid-side rotations. Locking is avoided by introducing an assumed linear shear strain field based on the tangential shear strains at the mid-sides. The element is free of spurious modes, satisfies the patch test and behaves correctly for thick and thin plate and shell situations. The element degenerates in an explicit manner to a simple DK form.

INTRODUCTION

Considerably effort has been put in recent years in the development of C_o continuous plate and shell elements valid for both thick and thin situations. A survey of recent work in this direction can be found in [1-3,9]. Despite of all these efforts there are not many elements that satisfy all the following "optimum" requirements:

a) Proper rank (no spurious modes for one element)
b) No shear locking
c) Satisfaction of constant curvature patch tests
d) Low sensitivity to distorsions
e) Good accuracy in displacements and stresses for thin and thick situations

f) Non dependence of artificial numerical factors
g) Simplicity of the formulation and of the programming

This paper presents a new triangular element which satisfies most (if not all) of above requirements. The displacement field is described by a standard C_o linear interpolation of the deflection in terms of the three corner values and a linear interpolation of the rotations in terms of the mid-side rotations. This introduces an incompatibility of the normal rotation along the sides of adjacent elements which however does not preclude satisfaction of the patch test. Shear locking is avoided by means of an assumed linear shear strain field in terms of the (constant) tangential shear values at the element mid-sides. This ensures fullfilment of the necessary compatibility conditions between the deflection, rotation and shear fields to guarantee the absence of locking in the thin limit [1-6].

The layout of the paper is the following. The basic equations of Reissner-Mindlin plate theory are briefly presented first. The finite element interpolation used is described next together with details of the derivation of the curvature and shear strain matrices. Examples of the good performance of the element proposed are presented for a range of plate and shell problems.The degeneration of the element to a simpler DK form involving 3 corner deflection values and 3 mid-side normal rotations is also briefly shown.

BASIC EQUATIONS OF REISSNER-MINDLIN PLATE THEORY

Figure 1 shows the geometry of a plate with the sign convention for the deflection w and the two independent rotations θ_x, θ_y.

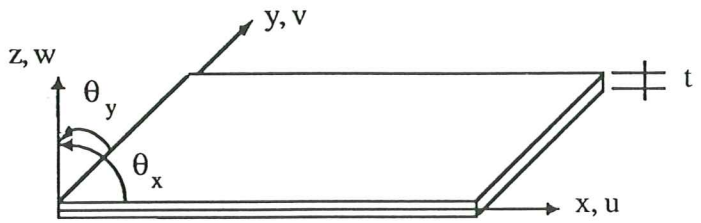

Figure 1 Sign convenion for displacement and rotations in a plate

Table I shows the basic equations of Reissner-Mindlin plate theory [1,2] defining the curvature and shear strain fields, the constitutive relationships and the equilibrium equation for a distributed loading q expressed by the Principle of Virtual Work (PVW).

Displacement field

$$\mathbf{u} = [w, \boldsymbol{\theta}^T]^T \quad , \quad \boldsymbol{\theta} = [\theta_x, \theta_y]^T$$

Curvature field

$$\boldsymbol{\chi} = [\chi_x, \chi_y, \chi_{xy}]^T = [-\frac{\partial \theta_x}{\partial x}, -\frac{\partial \theta_y}{\partial y}, -(\frac{\partial \theta_x}{\partial y} + \frac{\partial \theta_y}{\partial x})]^T$$

Shear strain field

$$\boldsymbol{\gamma} = [\gamma_x, \gamma_y]^T = [\frac{\partial w}{\partial x} - \theta_x, \frac{\partial w}{\partial y} - \theta_y]^T$$

Constitutive relationships

$$\mathbf{m} = [m_x, m_y, m_{xy}]^T = \mathbf{D}_b \boldsymbol{\chi}$$
$$\mathbf{s} = [Q_x, Q_y]^T = \mathbf{D}_s \boldsymbol{\gamma}$$

$$\mathbf{D}_b = \frac{Et^3}{12(1-\nu^2)} \begin{bmatrix} 1 & \nu & 0 \\ \nu & 1 & 0 \\ 0 & 0 & \frac{1-\nu^2}{2} \end{bmatrix} \quad , \quad \mathbf{D}_s = \alpha G t \begin{bmatrix} 1 & 0 \\ 0 & 1 \end{bmatrix} \ , \ \alpha = 5/6$$

Principle of virtual work

$$\int\int_A [\delta \boldsymbol{\chi}^T \mathbf{m} + \delta \boldsymbol{\gamma}^T \mathbf{s}] dA = \int\int_A \delta w q dA$$

Table I Basic equations of Reissner-Mindlin plate theory.

FINITE ELEMENT INTERPOLATION

Figure 2 shows the geometry of the triangular element proposed. The deflection field is linearly interpolated in terms of the three corner deflection values as

$$w = \sum_{i=1}^{3} L_i w_i \tag{1}$$

where $L_1 = 1 - \xi - \eta$, $L_2 = \xi$ and $L_3 = \eta$ are the shape functions of the standard linear triangle [1,2].

The rotation field is linearly interpolated in terms of the rotations at the element mid-sides as

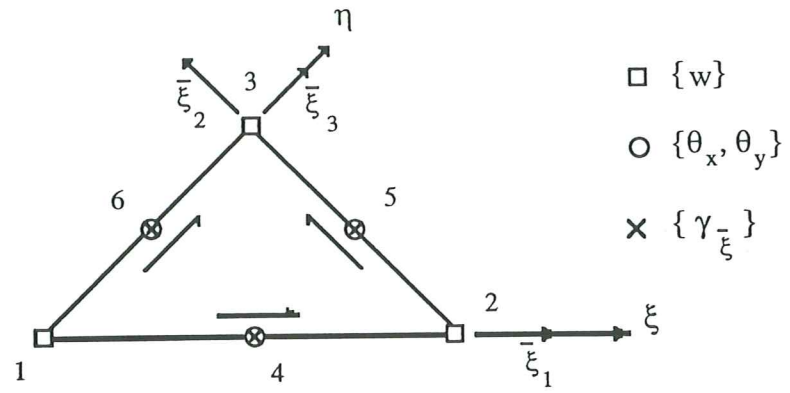

Figure 2 TLLL plate element. Geometric description and nodal variables

$$\boldsymbol{\theta} = \sum_{i=4}^{6} N_i \boldsymbol{\theta}_i \qquad , \qquad \boldsymbol{\theta}_i = [\theta_{xi}, \theta_{yi}]^T \tag{2}$$

where

$$\begin{aligned} N_4 &= 1 - 2\eta \\ N_5 &= 2\xi + 2\eta - 1 \\ N_6 &= 1 - 2\xi \end{aligned} \tag{3}$$

are the linear shape functions of nodes 4, 5 and 6.

Eqs (2) and (3) define an incompatible rotation field with side continuity enforced at the mid-side nodes only. The good performance of the element is ensured via satisfaction of the patch test as shown in the next section.

Curvature matrix

Substituting (2) into the curvature-rotation relationship of Table 1 leads to

$$\boldsymbol{\chi} = \mathbf{B}_b \mathbf{a} \tag{4}$$

with the nodal displacement vector defined as

$$\mathbf{a} = [w_1, w_2, w_3, \theta x_4, \theta y_4, \theta x_5, \theta y_5, \theta x_6, \theta y_6]^T \tag{5}$$

and the curvature matrix is given by

$$\mathbf{B}_b = [\underset{3\times 3}{\mathbf{0}}, \mathbf{B}_{b_4}, \mathbf{B}_{b_5}, \mathbf{B}_{b_6}] \;\; ; \;\; \mathbf{B}_{b_i} = \begin{bmatrix} -\frac{\partial N_i}{\partial x} & 0 \\ 0 & -\frac{\partial N_i}{\partial y} \\ -\frac{\partial N_i}{\partial y} & -\frac{\partial N_i}{\partial x} \end{bmatrix} \tag{6}$$

Note that $\mathbf{B}_{b_i}$ is constant for straight sided triangles.

Shear strain matrix

The assumed shear strain field is expressed in terms of the three tangential shear strains at the element mid-side points. After some algebra we can write in the natural coordinate system [6]

$$\boldsymbol{\gamma}' = \begin{Bmatrix} \gamma_\xi \\ \gamma_\eta \end{Bmatrix} = \begin{bmatrix} 1-\eta & -\sqrt{2}\eta & \eta \\ \xi & \sqrt{2}\xi & 1-\xi \end{bmatrix} \begin{Bmatrix} \gamma_{\bar{\xi}_1} \\ \gamma_{\bar{\xi}_2} \\ \gamma_{\bar{\xi}_3} \end{Bmatrix} = \mathbf{A}\hat{\boldsymbol{\gamma}}_{\bar{\xi}} \tag{7}$$

where $\gamma_{\bar{\xi}_1}$, $\gamma_{\bar{\xi}_2}$, $\gamma_{\bar{\xi}_3}$ are the tangential shear strains along sides 1-2, 2-3 and 1-3 respectively. The signs of the elements of **A** matrix in (7) correspond to the directions of side coordinates $\bar{\xi}_1$, $\bar{\xi}_2$ and $\bar{\xi}_3$ as shown in Figure 2 [6,10].

This shear strain interpolation coincides precisely with that used for the linear/quadratic plate triangles in refs. [5] and [6]. It can be easily checked that the chosen displacement and shear fields satisfy the *necessary conditions* for avoidance of locking defined as $n_w + n_\theta \geq n_\gamma$ and $n_\gamma \geq n_w$ where n_w, n_θ and n_γ are the number of available deflection, rotation and shear strain variables (after discounting the prescribed values). Further details on the variational justification of these inequalities can be found in [1,2,4-6,9].

The shear strain-displacement relationship is obtained by imposing along each side the condition $\gamma_{\bar{\xi}} - (\frac{\partial w}{\partial \bar{\xi}} - \theta_{\bar{\xi}}) = 0$ to be satisfied in a weighted integral form as

$$\int_{l_{ij}} W[\gamma_{\bar{\xi}} - \frac{\partial w}{\partial \bar{\xi}} + \theta_{\bar{\xi}}] d\bar{\xi} = 0 \tag{8}$$

The choice of a constant interpolation of the tangential shear strain along each side and a Galerkin weighting ($W = 1$) leads after appropiate substitution of (1) and (2) into (8) to

$$\hat{\boldsymbol{\gamma}}_{\bar{\xi}} = \begin{Bmatrix} \gamma_{\bar{\xi}_1} \\ \gamma_{\bar{\xi}_2} \\ \gamma_{\bar{\xi}_3} \end{Bmatrix} =$$

$$= \begin{bmatrix} -1 & 1 & 0 & x_{12} & y_{12} & 0 & 0 & 0 & 0 \\ 0 & -\frac{1}{\sqrt{2}} & \frac{1}{\sqrt{2}} & 0 & 0 & \frac{x_{23}}{\sqrt{2}} & \frac{y_{23}}{\sqrt{2}} & 0 & 0 \\ -1 & 0 & 1 & 0 & 0 & 0 & 0 & x_{13} & y_{13} \end{bmatrix} \mathbf{a} =$$

$$= \mathbf{C}\mathbf{a} \tag{9}$$

where $x_{ij} = x_i - x_j$, $y_{ij} = y_i - y_j$.

Combining (9) and (8) gives finally

$$\begin{Bmatrix} \gamma_x \\ \gamma_y \end{Bmatrix} = \mathbf{J}^{-1} \begin{Bmatrix} \gamma_\xi \\ \gamma_\eta \end{Bmatrix} = \mathbf{J}^{-1}\mathbf{A}\mathbf{C}\mathbf{a} = \bar{\mathbf{B}}_s\mathbf{a} \tag{10}$$

where **J** is the Jacobian matrix and

$$\bar{\mathbf{B}}_s = \mathbf{J}^{-1}\mathbf{A}\mathbf{C} \tag{11}$$

is the substitute shear strain matrix [2,6].

Stiffness matrix and equivalent nodal force vector

Substitution of (5) and (11) in the PVW expression of Table I leads to the standard form of the element stiffness matrix as

$$\mathbf{K}^{(e)} = \mathbf{K}_b^{(e)} + \mathbf{K}_s^{(e)} \tag{12}$$

where the bending and shear contributions are given by

$$\mathbf{K}_b^{(e)} = \int\int_{A^{(e)}} \mathbf{B}_b^T \mathbf{D}_b \mathbf{B}_b dA \tag{13}$$

$$\mathbf{K}_s^{(e)} = \int\int_{A^{(e)}} \bar{\mathbf{B}}_s^T \mathbf{D}_s \bar{\mathbf{B}}_s dA \tag{14}$$

The expression of the equivalent nodal force vector for a distributed loading of intensity q is given by

$$\mathbf{f}^{(e)} = \int\int_{A^{(e)}} \mathbf{N}^T q dA \qquad \text{with} \qquad \underset{3\times 9}{\mathbf{N}} = \begin{bmatrix} L_1 & & L_2 & & L_3 & \\ & \mathbf{0} & & \mathbf{0} & & \mathbf{0} \end{bmatrix} \tag{15}$$

Following the notation proposed in [6] the thick plate element presented here will be termed TLLL (for **T**riangle with **L**inear interpolation for the deflection, rotations and shear strain fields).

Remark 1. The exact integration of $\mathbf{K}_b^{(e)}$ and $\mathbf{K}_s^{(e)}$ for straight side triangles and homogeneous material requires 1 and 3 integration points, respectively.

Remark 2. Special case must be taken to handle the different number of degrees of freedom per node at equation solution and pre and postprocessing levels. Also the "a posteriori" computation of the rotation at corner nodes from the mid-side values for postprocessing purposes requires an adequate smoothing due to the incompatibility of the rotation field. Excellent results have been obtained in all cases by the authors using a simple nodal averaging procedure.

EXAMPLES

The performance of the TLLL plate element will be tested next for a number of plate problems.

1 Study of the element rank

An eigenvalue analysis shows that the element stiffness matrix, when exactly integrated, has only three zero eigenvalues for the whole range of thick and thin situations. The correctness of the element rank with respect to spureous mechanisms is therefore ensured.

The use of a reduced single point quadrature for the shear stiffness matrix introduces an extra zero eigenvalue. This invalidates, in principle, the use of this attractive simple quadrature for practical purposes. Preliminary numerical experiments show that this zero energy mode does not propagate in a a mesh, leading to accurate and very economical solutions. This encouraging result should be further validated before any definitive conclussion can be drawn. Exact integration is therefore used in all examples presented next.

2 Study of locking behaviour

Figure 3 shows the convergence of the central deflection value (normalized versus the Kirchhoff's solution) for a simple supported square plate ($a \times a$) under uniform loading. The same convergence curve is obtained for a range of thicknesses from thick to very thin situations. Similar results have been obtained for different plate problems (i.e., rectangular, circular, skew, etc.) with different boundary conditions, thus ensuring the absence of locking defects, as expected.

3 Patch tests

The following patch tests have been analyzed:

a) *Constant bending moment test* (Figure 4a)

A constant bending moment field ($M_x = M_y = M_{xy} = 1$) is obtained in all elements for this relatively thin case as expected.

b) *Cantilever plate under constant bending moment* (Figure 4b)

The element patch shown in Figure 4b with adequate boundary conditions was analized. The correct constant bending moment field and central deflection value was obtained (see Figure 4b).

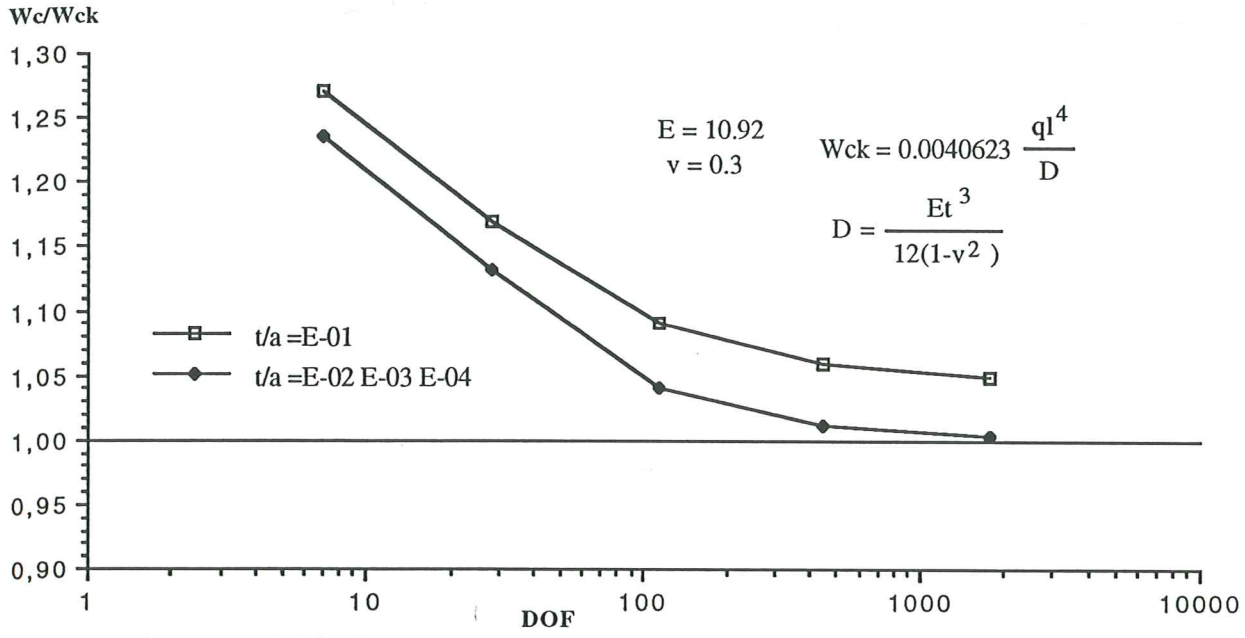

Figure 3 Simply supported square plate under uniform loading. Convergence of normalized central deflection value for thick and thin situations

c) *Twisting of a square plate* (Figure 4c)

We consider a thin square plate supported at three corners and subjected to a concentrated load at the fourth corner. Excellent agreement with the exact solution were obtained for all meshes analyzed (see Figure 4c).

d) *Constant shear patch test* (Figure 4d)

The geometry and boundary conditions for this patch test are shown in Figure 4d. A constant moment and shear field is obtained in the whole domain as expected.

Further details on the patch tests for the TLLL element can be found in [10].

4 Simply supported and clamped square plates under uniform loading

Table II shows the convergence of the central deflection and central bending moment M_x for thick ($t/a = 0.1$) and thin ($t/a = 0.01$) situations for a square plate with hard simple support conditions ($w = \theta_s = 0$). Numerical results are given for the two mesh orientations A and B shown in Figure 5. The same type of results are shown in Table III for the soft support ($w = 0$) case.

Table IV shows the convergence of the central deflection and central bending moment for the clamped case. Good results for thick and thin situations are obtained.

a) Constant bending moment test

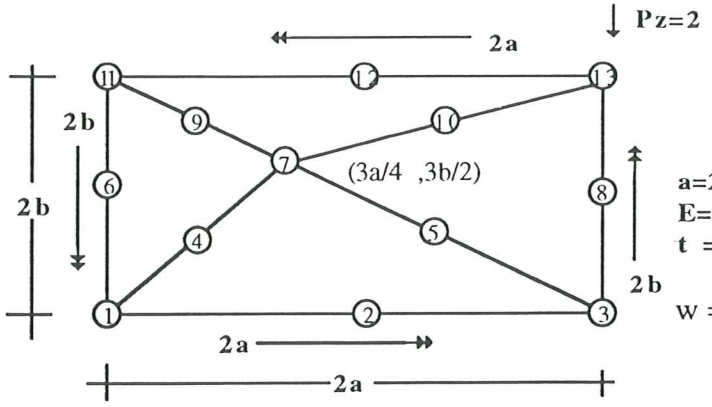

a=20 b=10
E=1000 v = 0.3
t = 1.0

w = 0 at nodes 1,3,11

Expected result
(for thin situations)

Mx = My = Mxy =1.0
in all points

b) Cantilever under constant bending moment

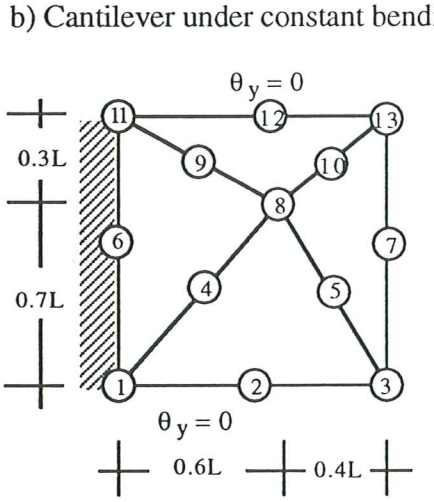

E=10.92
v=0.3
L=10
M=10

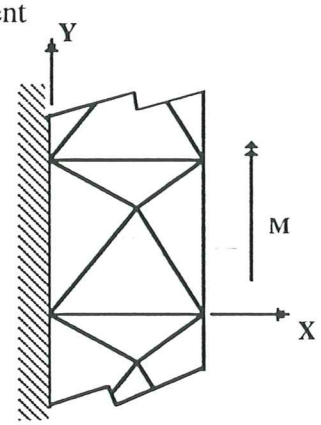

Expected result (for thin situations)

Mx = 1.0
My = 0.3
Mxy = 0.0
in all points.

Center deflection :$wEt^3 / Ml^2 = 5.46$

c) Square plate supported at three corners under point load

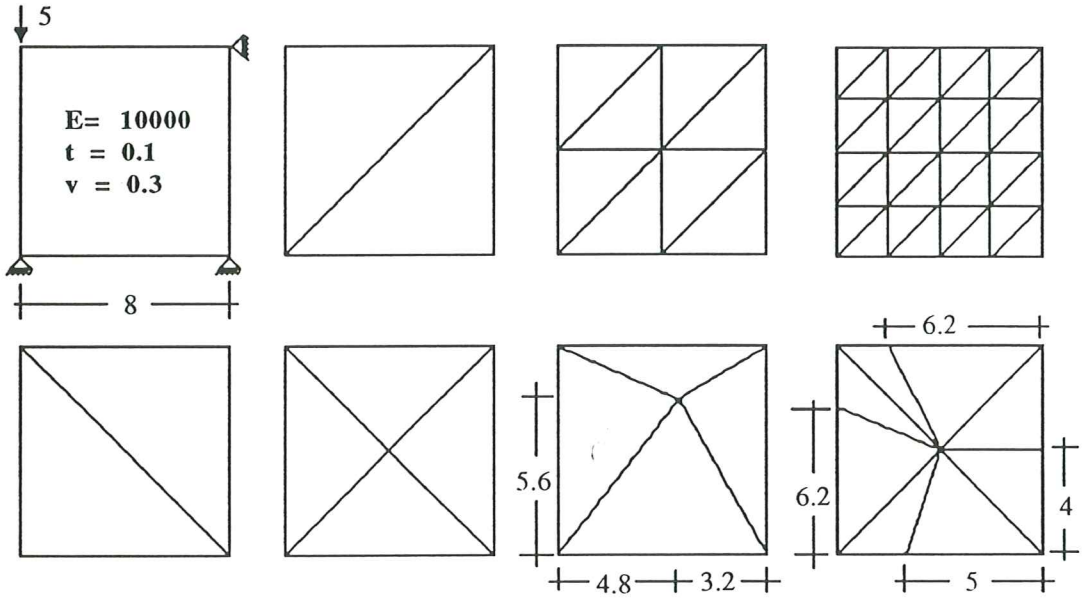

Expected result
(for thin situations)

Mx = 0.0
My = 0.0
Mxy = 2.5
in all points.

w= 0.0039 xy

Figure 4 Patch tests for TLLL element a) Constant bending moment test; b) Cantilever plate under constant bending moment; c) Square plate supported at three corners under point load

d) Constant shear patch test

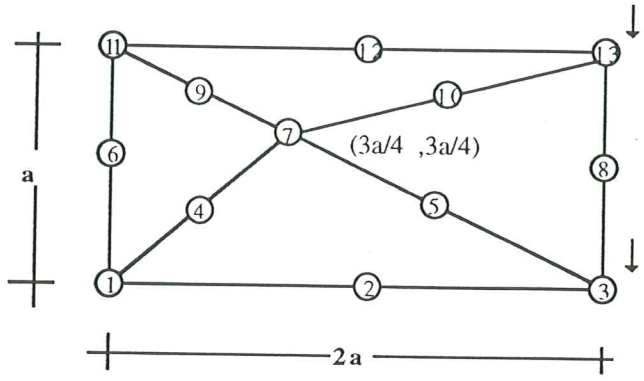

Expected result

Qxz =-1.0 in all points
Mx=My=Mxy=Qyz=0.0

w = 0.0 at nodes 1,11

$\theta_x = \theta_y = 0.0$ in all nodes

Figure 4 Patch tests for TLLL element d) Constant shear patch test

SIMPLE SUPPORTED SQUARE PLATE (HARD) UNDER UNIFORM LOADING NORMALIZED CENTRAL DEFLECTION					
		t/a = 0.1 (w x 10)		t/a = 0.01 (w x 10^4)	
MESH	DOF	A	B	A	B
2 x 2	7	5,1414	9,2607	5,0235	9,0212
4 x 4	28	4,7722	5,3477	4,5984	5,1294
8 x 8	112	4,4241	4,5252	4,2269	4,3184
16 x 16	448	4,3123	4,3302	4,1073	4,1271
32 x 32	1792	4,2826	4,2819	4,0753	4,0800
Analytic sol. [17]		4,2728		4,0623	
CENTRAL BENDING MOMENT					
		t/a = 0.1		t/a = 0.01	
MESH	DOF	A	B	A	B
2 x 2	7	1,3542	3,2689	1,3542	3,2827
4 x 4	28	3,7573	4,4632	3,7723	4,4583
8 x 8	112	4,5081	4,7149	4,5115	4,7119
16 x 16	448	4,7261	4,7636	4,7136	4,7739
32 x 32	1792	4,7901	4,7661	4,7688	4,7860
Analytic sol. [17]		4.79		4.79	

Table II Simply supported (hard: $w = \theta_s = 0$) square plate. Convergence of central deflection and central bending moment for thick ($t/a = 0.1$) and thin ($t/a = 0.01$) situations. Results given for mesh orientations A and B shown in Figure 5

5 Simply supported and clamped circular plates under uniform loading

Table V shows the convergence of the central deflection and central bending moment for circular plates with simply supported (soft: $w = 0$)

SIMPLE SUPPORTED SQUARE PLATE (SOFT) UNDER UNIFORM LOADING NORMALIZED CENTRAL DEFLECTION					
		t/a = 0.1 (w x 10)		t/a = 0.01 (w x 10^4)	
MESH	DOF	A	B	A	B
2 x 2	9	5,1557	9,3045	5,0237	9,0216
4 x 4	32	4,8427	5,4643	4,5592	5,1306
8 x 8	120	4,6088	4,7719	4,2292	4,3212
16 x 16	462	4,6350	4,7268	4,1125	4,1330
32 x 32	1824	4,6928	4,7723	4,0864	4,0918
Reference sol. [17]				4,0623	
CENTRAL BENDING MOMENT					
		t/a = 0.1		t/a = 0.01	
MESH	DOF	A	B	A	B
2 x 2	9	1,3690	3,2844	1,3543	3,2828
4 x 4	32	3,8279	4,5563	3,7731	4,4592
8 x 8	120	4,6825	4,9312	4,5136	4,7144
16 x 16	462	5,0275	5,1077	4,7183	4,7791
32 x 32	1824	5,1725	5,1907	4,7787	4,7964
Reference sol. [17]				4.79	

Table III Simply supported (soft: $w = 0$) square plate. Convergence of central deflection and central bending moment for thick ($t/a = 0.1$) and thin ($t/a = 0.01$) situations. Results given for mesh orientations A and B shown in Figure 5

and clamped edges. Good convergence to existing analytical solutions [7] is obtained for thick and thin situations.

6 Cantilever skew plates under uniform loading

Table VI shows the convergence of the central deflections at the two free corners (Figure 5) for different cantilever skew plates under uniform loading. Good convergence to the numerical solutions obtained with alternative triangular elements [12,13] is obtained in all cases. Note however that the element shows a slightly stiffer behaviour than the elements presented in these references (in particular for high skew angles). This is compensated by the bigger simplicity of the element here proposed.

EXTENSION TO SHELL ANALYSIS

The TLLL plate element presented in previous sections has been successfully combined with the simple linear plane stress triangle [1, 2] for linear and non linear shell analysis. The linear shell formulation is based in the standard facet shell approach. Two rotational degrees of freedom at the mid-nodes are kept which makes the formulation applicable to smooth shells only. The extension for kinked shell situations requires the introduction of a third drilling rotation at the non-coplanar nodes in the standard manner [1,

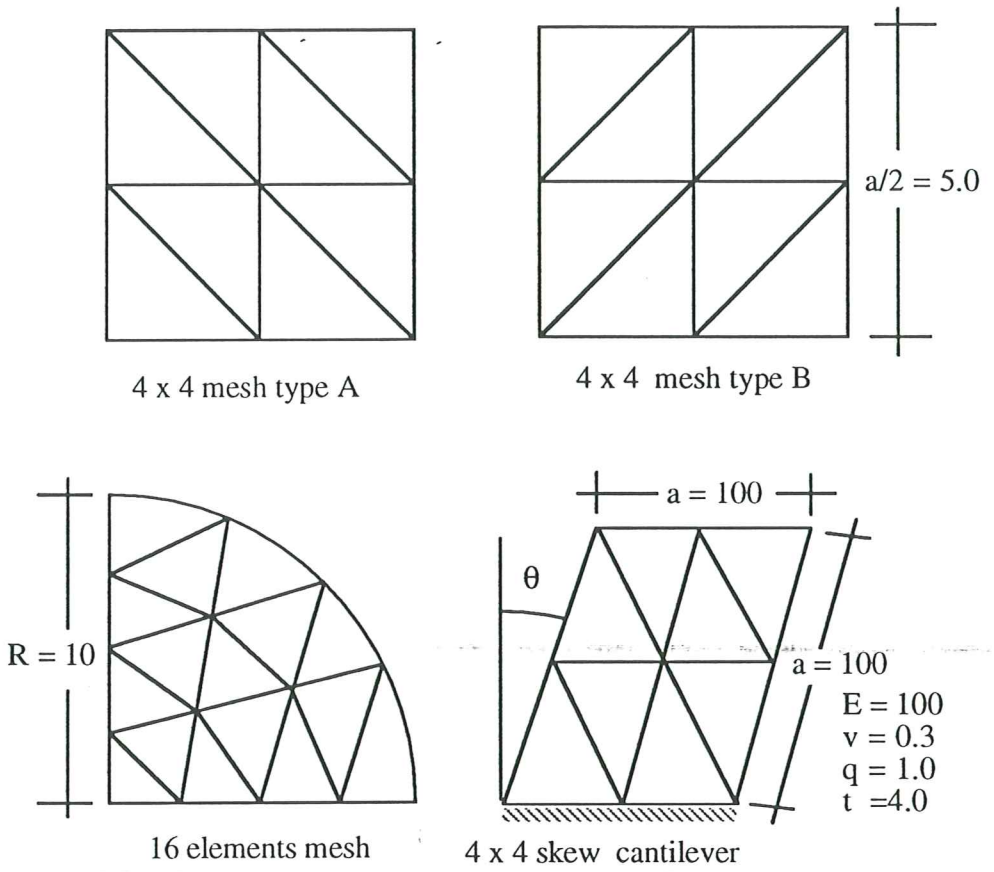

Figure 5 Description of meshes used for the analysis of square, circular and skew plates in Examples 4-6

2]. The non linear shell formulation is based in Simo's shell theory [15,16].

Figure 6 shows an example of the good performance of the TLLL element for non linear shell analysis. The example corresponds to a pinned shallow cilyndrical panel subjected to a central load. The geometry of the panel and the material properties are shown in Figure 6a. Increasing values of the applied load lead, eventually, to snap-through of the panel and reversal of its curvature. This problem is analyzed using different meshes on one quadrant using symmetry conditions for two different thickness: $R/t = 200$ and $R/t = 400$. The load deflection paths for these cases are shown in Figures 6a and 6b. Arc length control was necessary in the second case due to the complexity of the different solution paths. Numerical results agree well in all cases with those reported in [16].

Further evidence of the good performance of the TLLL element for shell analysis can be found in [10,11].

CLAMPED SQUARE PLATE UNDER UNIFORM LOADING NORMALIZED CENTRAL DEFLECTION					
		t/a = 0.1 (w x 10)		t/a = 0.01 (w x 10^4)	
MESH	DOF	A	B	A	B
2 x 2	7	4,6284	7,7073	4,5106	7,4432
4 x 4	24	2,8125	3,1095	2,6264	2,8566
8 x 8	104	1,8861	1,9508	1,6656	1,6985
16 x 16	432	1,6076	1,6424	1,3727	1,3811
32 x 32	1760	1,5344	1,5634	1,2946	1,2970
Analytic sol. [17]		1,4990		1,2653	
CENTRAL BENDING MOMENT					
		t/a = 0.1		t/a = 0.01	
MESH	DOF	A	B	A	B
2 x 2	7	0,8207	2,0592	0,8207	2,0831
4 x 4	24	1,9297	2,4246	1,9562	2,4211
8 x 8	104	2,1796	2,3841	2,2097	2,3457
16 x 16	432	2,2476	2,3619	2,2670	2,3120
32 x 32	1760	2,2728	2,3506	2,2835	2,2980
Analytic sol. [17]		2.31		2.31	

Table IV Clamped square plate. Convergence of central deflection and central bending moment for thick ($t/a = 0.1$) and thin ($t/a = 0.01$) situations. Results given for mesh orientations A and B shown in Figure 5

Derivation of a 6 DOF Discrete-Kirchhoff triangle

A simple Discrete Kirchhoff (DK) triangle can be derived from the TLLL plate element presented in previous section simply by constraining the mid-side shear strains to a zero value. This provides the following relationship between the tangential rotation along a side ij and the two nodal deflection values corresponding to the side as

$$\theta_s^{ij} = \frac{w_j - w_i}{l_{ij}} \tag{16}$$

The resulting DK triangle termed DKTLL (for **D**iscrete **K**irchhoff **T**riangle with **L**inear deflection and **L**inear rotation fields) has only 6 DOF (three corner deflection and three normal rotation at the element mid-sides). The element stiffness matrix involves now the flexural contribution only (eq. (13)). The explicit form of the modified curvature matrix is shown in Table VII. Note that a single point quadrature suffices for exact evaluation of $\mathbf{K}_b^{(e)}$ over straight side triangles with homogeneous material properties.

CLAMPED CIRCULAR PLATE UNDER UNIFORM LOADING NORMALIZED CENTRAL DEFLECTION AND BENDING MOMENT					
		t/R = 0.1		t/R = 0.01	
ELEM	DOF	Wc x 10^2	(Mx)c	Wc x 10^5	(Mx)c
4	12	3,7668	6,9599	3,6950	6,9606
16	54	2,2352	7,7235	2,1657	7,7431
64	220	1,7882	7,9751	1,7186	8,0146
144	498	1,7023	8,0243	1,6326	8,0726
225	780	1,6774	8,0391	1,6077	8,0904
Reference sol.[7,17]		1,6339	8,1250	1,5625	8,1250
SIMPLED SUPPORTED CIRCULAR PLATE (SOFT) NORMALIZED CENTRAL DEFLECTION AND BENDING MOMENT					
		t/R = 0.1		t/R = 0.01	
ELEM	DOF	Wc x 10^2	(Mx)c x 10	Wc x 10^5	(Mx)c x 10
4	17	7,2815	1,6400	7,2096	1,6402
16	62	6,7248	1,9427	6,6553	1,9449
64	236	6,5191	2,0279	6,4495	2,0319
144	522	6,4763	2,0437	6,4066	2,0487
225	810	6,4637	2,0484	6,3939	2,0536
Reference sol.[7,17]		6,4416	2,0625	6,3702	2.0625

Table V Clamped and Simply supported (soft: $w = 0$) circular plates. Convergence of central deflection and central bending moment for thick and thin situations

CANTILEVER SKEW PLATE UNDER UNIFORM LOADING NORMALIZED DEFLECTION AT CORNER NODES w x (Et^3/qa^4)							
		20°		40°		60°	
MESH	DOF	W1	W2	W1	W2	W1	W2
2 x 2	14	3,0093	2,6744	2,5112	1,3772	2,1821	0,4959
4 x 4	41	1,9701	1,7478	1,7478	0,8321	1,3882	0,2940
8 x 8	137	1,6032	1,1611	1,3950	0,6349	1,0800	0,2111
16 x 16	497	1,4802	1,0741	1,2610	0,5724	0,9521	0,1781
32 x 32	1889	1,4442	1,0517	1,2159	0,5554	0,9030	0,1672
DRM [12] 416 DOF		1,4269	1,0436	1,1789	0,5456	0,8435	0,1553
EL1[12,13] 472DOF		1,4237	1,0421	1,1722	0,5441	0,8314	0,1538

Table VI Cantilever rectangular skew plates. Convergence of the central deflection at the two free corners for different skew angles

Remark 3. The stiffness matrix of the DKTLL element coincides with that the well known Morley's thin triangular plate element [8] and also with that

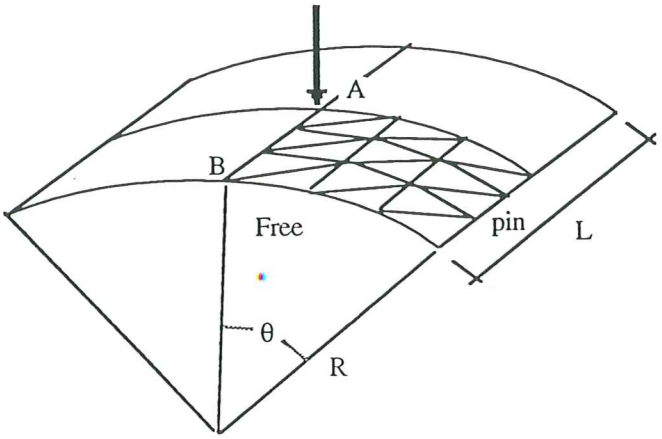

E=3102.7 N/mm ^{2}
v = 0.3
R = 2 540 mm
L = 254 mm
t =12.7 / 6.35 mm
θ = 1 rad.

Point Mesh:
A B
8 x 8 : 159 DOF
12 x 12 : 347 DOF
16 x 16 : 607 DOF

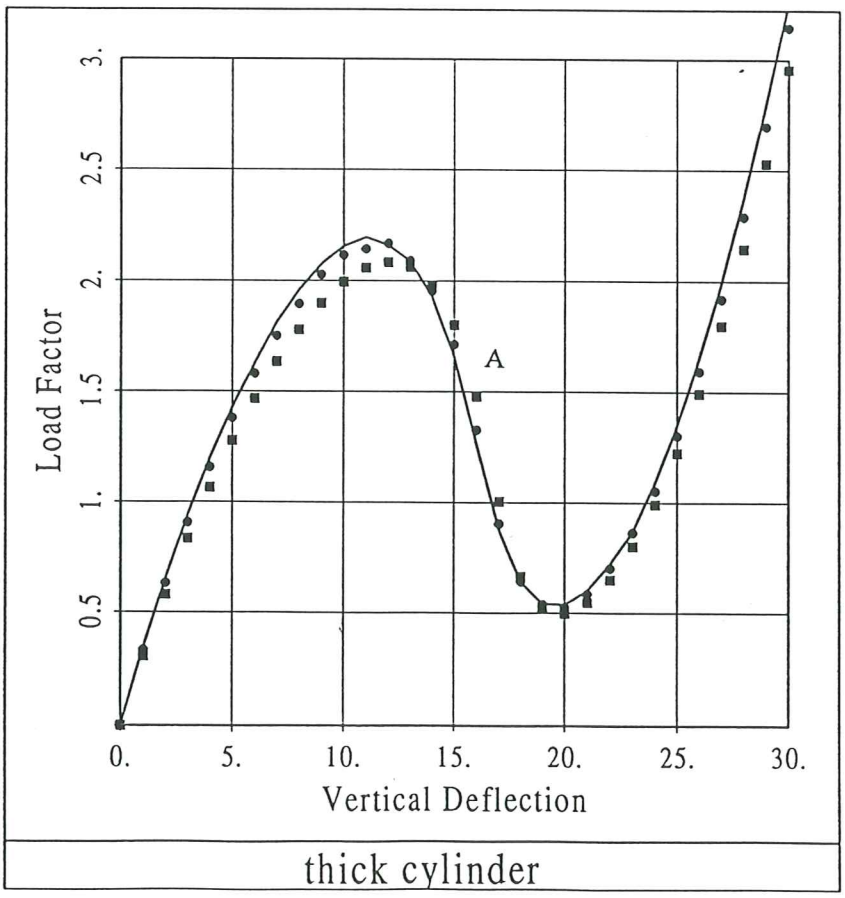

Figure 6 a) Problem definition of the snap through of a shallow hinged cylindrical panel; b) Load deflection path for the $R/t = 200$ case. Displacement control using 30 step levels are used

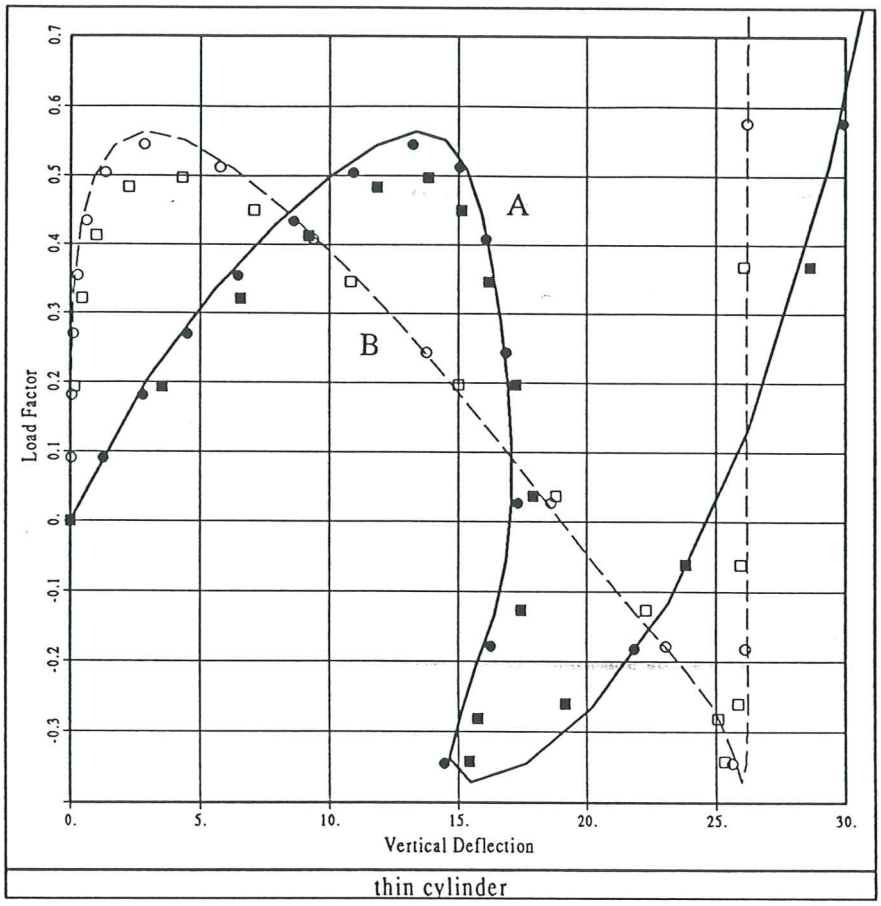

Figure 6 c) Load-deflection path for the $R/t = 400$ case. Arc-length control was necessary in this case. 20 step levels were used

of the HSM6 triangle proposed by Batoz and Dhatt (see pages 375 and 390 of Vols I and II of [9], respectively). However, the derivation presented here follows a completely different and simpler procedure. Also, note that the equivalent nodal load vector is different for each of these cases. The acuracy of the DKTLL element is identical to that shown for the TLLL element for thin plate situations in previous examples.

Remark 4. An extension of the DKTLL element to account for transverse shear deformation effects has been recently proposed by Van Keulen [7]. The approach is based on the introduction of three tangential shear strains at the element mid-side points wich remain as additional variables.The final discretized system of equations is derived via a mixed-hybrid approach. Futher details can be found in [7].

$$\mathbf{B}_b = \begin{bmatrix} (a_{12}-a_{13}) & (a_{23}-a_{12}) & (a_{13}-a_{23}) & c_{12} & c_{23} & -c_{13} \\ (a_{13}-a_{12}) & (a_{12}-a_{23}) & (a_{23}-a_{13}) & b_{12} & b_{23} & -b_{13} \\ (d_{13}-d_{12}) & (d_{12}-d_{23}) & (d_{23}-d_{13}) & -2a_{12} & -2a_{23} & 2a_{13} \end{bmatrix}$$

$$a_{ij} = \frac{x_{ij}y_{ij}}{l_{ij}^2} \quad ; \qquad b_{ij} = \frac{x_{ij}^2}{l_{ij}} \quad , \qquad c_{ij} = \frac{y_{ij}^2}{l_{ij}}$$

$$d_{ij} = \frac{x_{ij}^2 - y_{ij}^2}{l_{ij}^2} \quad ; \quad x_{ij} = x_i - x_j \quad , \quad y_{ij} = y_i - y_j$$

$$l_{ij} = (x_{ij}^2 + y_{ij}^2)^{1/2}$$

Table VII Curvature matrix of DKTLL triangle.

CONCLUDING REMARKS

A simple 9 DOF triangular plate element with linear displacement and rotation fields has been presented. The element seems to satisfy all requirements defining an "optimum" plate element valid for thick and thin situation. The drawback of having a different number of degrees of freedom per node as well as that of its slightly over-stiff behaviour are compensated by the simplicity of the element formulation. Preliminary results obtained show that the element is also very adequate for shell analysis.

Current research work aims to enhance the convergence behaviour of the element so that it can favourably compete with other low order triangles recently proposed for plate and shell analysis [3-7,12,14].

ACKNOWLEDGEMENTS

F. Zarate gratefully acknowledges the support of the Government of Mexico during the development of this work.

F. Flores is supported by a fellowship from the Spanish Government, this support is gratefully acknowledged.

REFERENCES

1. Zienkiewicz, O.C. and Taylor R.L., *The finite element method*, Mc.Graw Hill, Vol. I, 1990; Vol. II, 1991.

2. Oñate, E., *Structural Analysis by the Finite Element Method*, CIMNE, Barcelona, 1994.
3. Batoz, J.L. and Katili, I., "On a simple triangular Reissner-Mindlin plate element based on incompatible modes and discrete constraints", *Int. J. Num. Meth. Engng.*, **35**, 1603-32, 1992.
4. Zienkiewicz, O.C. and Lefebvre, D., "A robust triangular plate bending element of Reissner-Mindlin type", *Int. J. Num. Meth. Engng.*, **26**, pp. 1169-1184, 1988.
5. Zienkiewicz, O.C., Taylor, R.L., Papadopoulos, P. and Oñate, E., "Plate bending elements with discrete constraints: New triangular elements *Computer and structures*", Vol. **35**, 505-522, 1990.
6. Oñate, E., Zienkiewicz, O.C., Suarez, B. and Taylor, R.L., "A methodology for deriving shear constrained Reissner-Mindlin plate elements", *Int. J. Num. Meth. Engng.*, Vol. **33**, N° 2, pp. 345-367, Jan. 1992.
7. Van Keulen, F., "On refined triangular plate and shell elements", *Ph D. Thesis*, Technische Universiteit Delft, January, 1993.
8. Morley, L.S.D., "On the constant moment plate bending element", *J. Strain Anal.*, Vol. **6**, pp. 20-24, 1971.
9. Batoz, J.L. and Dhatt, G., "Modelisation des structures par elements finies", HERMES, Paris, Vol. 2 "Poutres et Plaques", 1990; Vol. 3 "Coques", 1992.
10. Zarate, F., "Nuevos elementos finitos para análisis de placas y láminas" *Ph.D. Thesis* (In Spanish), UPC, Barcelona, (to be submitted).
11. Flores, F. and Oñate, E., "A comparison of different finite elements based on Simo's shell theory", Research Report, N. 33, CIMNE, Barcelona, 1993.
12. Auricchio, F. and Taylor, R.L., "3 node triangular elements based on Reissner-Mindlin plate theory", Report no. UCB/SEMM-91/04, Dpt. Civil Engng., Univ. of California, Berkely, May 1991.
13. Xu, Z., "A thick-thin triangular plate element", *Int. J. Num. Meth. Engng.*, **33**, 963-73, 1992.
14. Zienkiewicz, O.C., Auricchio, F. and Taylor, R.L., "Linked interpolation for Reissner-Mindlin plate elements", to be published in *Int J. Num. Meth. Engng.*
15. Simo, J.C. and Fox, D.D., "On a stress resultant geometrically exact shell model. Part I. Formulation and optimal parametrization", *Comp. Meth. in Appl. Mech. and Engng.*, **72**, 267-304, 1989.
16. Simo, J.C. Fox, D.D. and Rifai, M.S., "On a stress resultant geometrically exact shell model. Part III. Computational aspects of the non linear theory", *Comp. Meth. in Appl. Mech. and Engng.*, **79**, 21-70, 1990.
17. Timoshenko, S. and Woinowsky-Krieger, S., "*Theory of plates and shells*". Mac.Graw Hill, New York, 1959.

LIST OF FIGURES

LIST OF TABLES

El Método de los Elementos Finitos

Cuarta Edición

Volumen 1

Formulación básica y problemas lineales